Effects on the loading of horizontal axis turbines when operating under wave and currents

Rodrigo Martinez, Stephanie Ordonez-Sanchez, Matthew Allmark, Cameron Johnstone, Tim O'Doherty, Catherine Lloyd, Gregory Germain, Benoit Gaurier

Abstract—**Tidal turbines are still at an early deployment stage compared to other renewable sources. In order to achieve a commercial stage, a full understanding of the hydrodynamic loadings that influence a tidal turbine is needed. This understanding will aid reduce uncertainties related to the turbine performance and its structural and mechanical response to the environment. Wave-induced loadings are of key concern for determining blade and drive train design loads and the fatigue life of components. In a real sea state, waves have an irregular nature that could potentially add complexity to the loading patterns. The use of different control strategies was opted to understand the turbine's behaviour under the same flow conditions and potentially, mitigate loading fluctuations. To investigate these aspects, a set of laboratory tests was conducted in a recirculating wave and current tank at IFREMER, Boulogne-Sur-Mer, France. A 0.9 m diameter three bladed horizontal axis turbine model was tested under flow only and combined wave and current with regular and irregular waves at a range of tip-speed-ratios. Rotor thrust, torque and blade root bending moment were measured. It was observed that mean loads and power capture values were not affected by the control strategy nor the addition of waves. However, using torque control resulted in increased thrust fluctuations of up to 75% the mean value. At the same tip-speed-ratio, thrust fluctuations were only 40% off the mean value under speed control.**

Keywords—**Dynamic loading, irregular waves, tidal turbine, recirculating tank, wave-current interaction.**

I. Introduction

The influence of wave-induced loads is an aspect as important to consider as loads induced by current-only in the design and operation of tidal turbines. It has been experimentally observed (e.g. [1]–[8]) that the wave-induced loads influence the peak loads seen by the turbine. In addition, the dynamic nature of these loads are responsible of fluctuations on the turbine loads up to 2-3 times the average values ([1]). Also, [9] demonstrated that the wave-induced fluctuating loads cause eccentric loading on the bearings and [10] quantified the effect of these fluctuations on the fatigue life of the blades. Understanding these fluctuations will help with power conditioning and integration with the electricity grid. Recent studies have begun to address load fluctuations through numerical simulations studies too (e.g. [11]–[13])

One of the main gaps between experimental studies and the flow conditions experienced in the field is that the majority of tests conducted have been with regular waves. However, it is unlikely that waves will be regular in a real sea state. Another gap is that in laboratory studies, speed control is predominantly used to keep a constant rotational speed independently of the flow condition in order to optimize power capture. However, in most full scale turbines the use of variable speed and torque control is preferred.

The aim of this work is to investigate these two gaps in knowledge. It is expected that the data and analysis obtained from these tests and study will be of useful input when designing mechanical and structural components of a turbine and for numerical and CFD validations.

This work forms part of a wider EPSRC project entitled 'Dynamic Loadings on Tidal Turbine Arrays' lead by Cardiff University. The first set of experimental tests conducted as part of this project were presented on [14] and [15], in which regular and irregular wave forms were tested under both speed and torque control modes at a towing tank. The present study, based on the original flow conditions, aims to build up on the results from said experimental campaign. This new set of experimental tests provided the data to compare the turbine behaviour under the same conditions in a recirculating tank.

II. Methodology

The laboratory experiments presented in this work were conducted at the 4 x 2 x 18 m wave and current tank flume at IFREMER, Boulogne-Sur-Mer, France over a two-week

ID 1440 track TDD
This work was supported by the EPSRC under grant EP/N020782/1

Martinez, R., Ordonez-Sanchez, S. and Johnstone, C. are with the University of Strathclyde, 16 Richmond St. Glasgow, G1 1XQ. (e-mail: r.martinez@strath.ac.uk).

Allmark, M., O'Doherty, T. and Lloyd, C. are with Cardiff University, Cardiff, CF10 3AT

Germain, G. and Gaurier, B. are with IFREMER, Centre Manche Mer du Nord - 150, Quai Gambetta - 62200 Boulogne-sur-Mer.

period in April 2018. The test set-up, programme and measurement systems are detailed below.

A. Test set-up

For the tests, the turbine was attached from a 0.105 m diameter stanchion to a structure above the flume tank. Details of the model turbine design are given in Section II.C. Figure 1 shows the turbine installed on the flume. The Laser Doppler Velocimetry (LDV) beam can be seen upstream of the turbine. The turbine hub centre was set 1 m below the still water surface, and centred in the cross stream direction. Cables from the turbine ran along the inside of the stanchion and connected to the control and data acquisition systems situated next to the tank. The turbine and flow measurement systems are detailed in Section II.D and II.E, respectively.

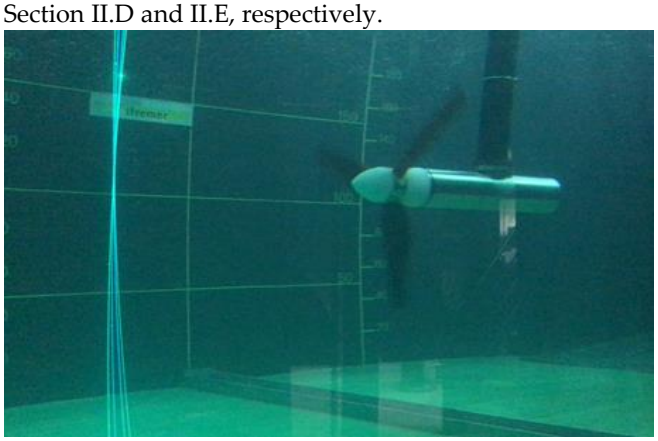

Figure 1 Image of tank setup

B. Test programme and procedures

The test programme consisted of current only, regular and irregular wave-current cases. The flow speed was set equal in each case, and was designed to provide approximately Reynolds independent conditions. Wave parameters were set to match those used in [14] and [15]. The regular wave height and frequency were matched with the significant wave height and minimum frequency of the irregular waves, $H=H_S$ and $F=F_{min}$ respectively. A Jonswap spectrum was used for the irregular waves. Table I shows the prescribed test parameters.

Each flow condition was tested in torque and speed control. For each flow condition, the turbine was operated at a range of tip-speed-ratios (TSR). The torque control levels were selected from the average torque measurements under speed control for each TSR.

Prior to any flow condition change, a recording of the turbine's instrumentation was taken with the turbine stopped, no waves and no current. These tests allow to check for any inconsistency or change that could have happened between tests.

TABLE I
DESIGN PARAMETERS

Case	Test type	Wave type	Flow speed [m/s]	Wave height [m]	Wave freq. [Hz]	Control type
Current	C	N/A	1.0	N/A	N/A	Speed
SC-W_{REG}	W-C	Regular	1.0	0.19	0.7	Speed
TC-W_{REG}	W-C	Regular	1.0	0.19	0.7	Torque
SC-W_{JSP}	W-C	Irregular	1.0	0.19	0.7	Speed
TC-W_{JSP}	W-C	Irregular	1.0	0.19	0.7	Torque

A trigger between the turbine and tanks data acquisition systems would initialise logging of the data simultaneously. All the data from the turbine's instrumentation and flow measurement instruments was sampled at 100 Hz, whereas the motor data was sampled at 28 Hz.

C. Model turbine design

The turbine model used in this experiments was the horizontal axis, 0.9 m diameter 3-bladed model developed in [16]. The turbine is controlled by a Bosch Rexroth motor and drive along with an encoder to close the control loop. LabVIEW was used for the control algorithms to keep a desired constant speed or torque.

The blades were designed for optimum power capture. The design was based on a Wortmann FX 63-137 profile from previous studies ([17], [18]). A Blade Element Momentum Theory model was used to optimise the design of the blades' twist, pitch and chord. Further details on the blade design can be seen in [19].

D. Turbine measurement equipment

For logging the turbine loadings, an Applied Measurements thrust and torque transducer was fitted between the rotor hub and the dynamic seals. Applied Measurements provided calibrations for thrust and torque. Previously mentioned tests (Section II.B) where the turbine was stationary and the water was still, were performed to correct for the offset on the readings. This constant was then used to zero the readings, along with the calibration gradient supplied by the manufacturer.

Measuring out-of-plane bending moment was possible with strain gauges mounted on each of the blade roots. However, due to some waterproofing issues, data from blade 1 was lost towards the end of the testing period. The similarity between blade 2 and blade 3 was so close to each other that in this work only the measurements from the root of blade 3 are discussed.

E. Flow and wave measurements

The wave height was measured with a resistive wave gauge placed in-line with the turbine's rotor in the cross-stream direction at 0.78m from the centre of the rotor.

For the regular waves, an average wave height of 0.17 m was recorded, 0.02 m below the input value. The standard deviation of the wave height was of 0.002 m between tests.

The average wave frequency was 0.69 Hz, with a standard deviation of 0.0001 s between tests.

For the irregular wave tests, the zero up-crossing method was used to define each wave period. Then, wave height and frequency was calculated for each individual period. These properties are given in Table 2.

According to the design parameters from Table I, the wave height and frequency of the regular waves are equal to the significant wave height and minimum frequency of the irregular waves ($H=H_S$ and $F=F_{min}$). However, looking at Table 2, $H \neq H_S$ and $F \neq F_{min}$. Perhaps, the duration of the tests didn't allow for the full spectrum to develop or an issue with the facility prevents the values to match. For ease of referencing, the design parameters will be used herein.

TABLE II
WAVE HEIGHT AND FREQUENCY PROPERTIES OF IRREGULAR WAVES USING ZERO UP-CROSSING METHOD

Repeats	1	2	3	4	5	6
Duration of test	300	300	300	300	300	300
Mean frequency [Hz]	0.74	0.73	0.73	0.73	0.75	0.75
Max frequency [Hz]	1.82	1.85	1.92	1.89	1.85	1.92
Min frequency [Hz]	0.46	0.46	0.47	0.33	0.38	0.48
Mean height [m]	0.07	0.07	0.07	0.07	0.07	0.07
Max height [m]	0.15	0.15	0.14	0.14	0.15	0.15
Min height [m]	0.01	0.02	0.02	0.02	0.02	0.02
Significant height [m]	0.10	0.10	0.10	0.10	0.10	0.10

Although the irregular waves are somewhat arbitrary in nature, they still provide an insight on the wave-induced dynamic loadings on the turbine They will provide a starting point of comparison between the effects of random and regular waves on the turbine.

Flow speed was monitored with an LDV current meter mounted 1 m up stream of the turbine at different cross stream positions and an Acoustic Doppler Velocimetry (ADV) current meter was mounted in line with the rotor at 1.05 m from the centre of the rotor at hub height.

The data presented herein are based on the ADV data as it doesn't change positions between tests, making it possible to compare the data from run to run.

III. RESULTS AND DISCUSSION

The results measured from the turbine's instrumentation are discussed in this section, firstly as time-averaged performance, secondly as load fluctuations caused by waves and lastly as phase misalignment between signals.

A. *Average performance*

The turbine's power and thrust coefficients, C_P and C_T respectively, are shown in Figure 2 and 3 for all flow conditions and control modes. These are plotted against tip speed ratio (TSR). For further details on these standard parameters see [20]. The data for blade 3's root bending moment for all the cases against TSR is shown in Figure 4. In terms of the measurement quality, the low scatter in the data in Figure 2-4 indicates qualitatively that the results are of acceptable quality. The standard deviation between available repeat tests was less than 1.5% of the mean value for C_T and root bending moment and 3% for C_P. These values demonstrate that the chosen instrumentation and methodologies were appropriate for these experiments.

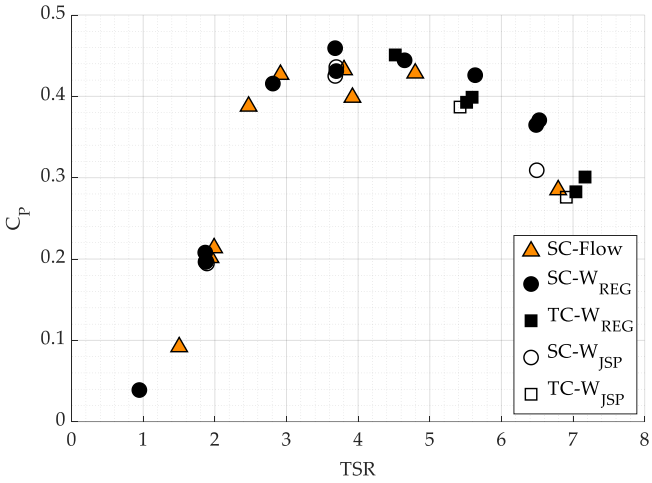

Figure 2 Mean power coefficient (C_P) against tip-speed-ratio (TSR) for all cases.

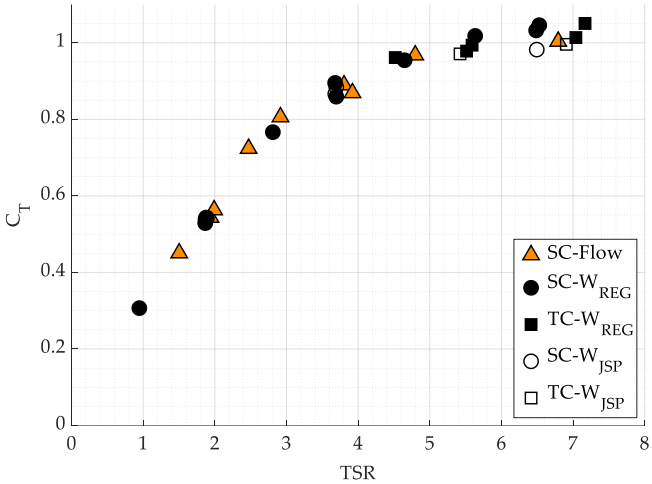

Figure 3 Mean thrust coefficient (C_T) against tip-speed-ratio (TSR) for all cases.

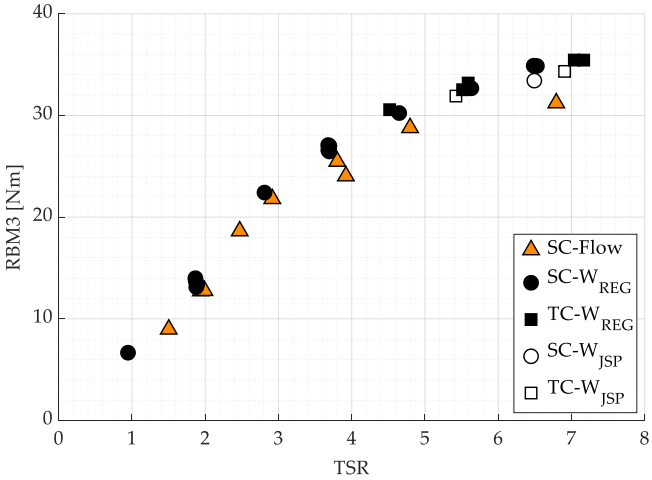

Figure 4 Mean root bending moment (RBM) of blade 3 against tip-speed-ratio (TSR) for all cases.

For tests under speed control, the rotational speed was kept constant. In these tests, the standard deviation in the

rotational speed (Figure 5) was found to decrease as TSR increase from a maximum of 2.2% (TSR=1) to a minimum of 0.6% (TSR=7). The average rotational speed was not affected by running waves.

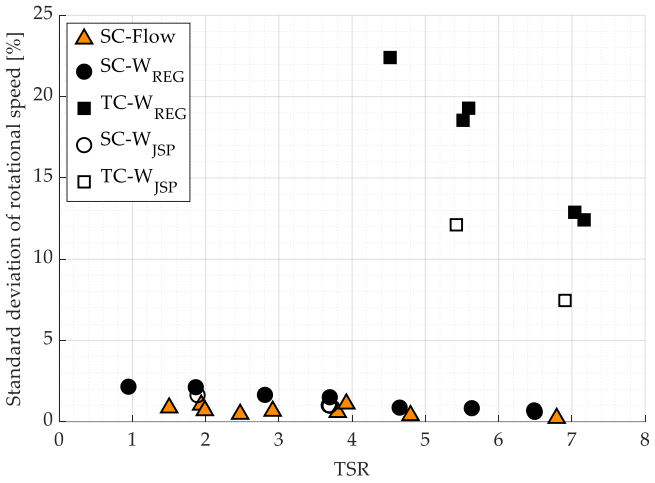

Figure 5 Standard deviation of rotational speed as a percentage of the mean values against tip-speed-ratio (TSR) for all cases.

In the few torque control tests (Figure 6), the standard deviation is increased as the TSR increased, with a minimum of 2% at TSR=4.5 and a maximum of 7% at TSR=7of the mean torque, and similarly to the speed control cases, average values were not influenced by the addition of waves.

In Figure 5 the standard deviation of the rotational speed in the torque control cases decreases with TSR. Comparing it to the speed control cases, it is up to 30 times larger. Similarly, in Figure 6, the standard deviation of torque in the speed control cases is up to 15 times larger than in the torque control cases.

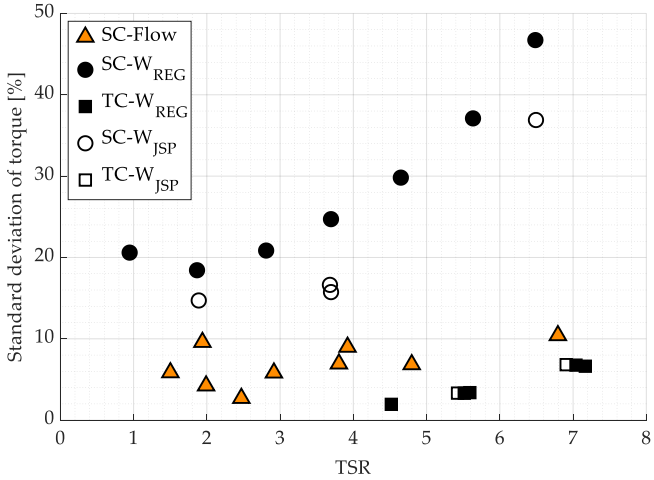

Figure 6 Standard deviation of torque as a percentage of the mean values against tip-speed-ratio (TSR) for all cases.

In Figure 2, 3 and 4 the agreement between tests under the same flow condition in both torque and speed control is tight. This agreement indicates that neither the control mode nor the addition of waves have a significant influence in the average values of power, thrust or blade root bending moment.

B. Loading fluctuations

In the previous section, it was observed that regardless of the control strategy or the addition of waves the average values remained unaffected.

In this section results of analysing the loading fluctuations in the time domain is presented. This analysis was performed to have a better understanding of the frequency and amplitude of these loading fluctuations as they play an important role in power control, grid integration and structural design of the different mechanical components that comprise a turbine.

When observing the structural loading patterns, it is clear that the largest influence in their fluctuations is the wave-induced loads, with predominately a single fluctuation occurring each wave period.

In Figure 7, 8 and 9 the average loading ranges (a) are presented along with the average maximum and minimum values (b) against TSR for each test.

The size of the fluctuations on the rotational speed are shown in Figure 7a. In the torque control cases, the rotational speed decreases as the TSR increases, but both maximum and minimum speed increase as TSR increases (Figure 7b). The fluctuation range for the torque control cases is up to around 70% of the mean speed for regular waves and 30% for irregular waves. For the speed control cases, including flow only cases, the rotational speed range is kept well below 5%.

The gap between maximum and minimum values is of over 100 RPM for the torque control cases and around 10 RPM for the speed control cases. The irregular wave cases show a smaller range than the regular wave cases.

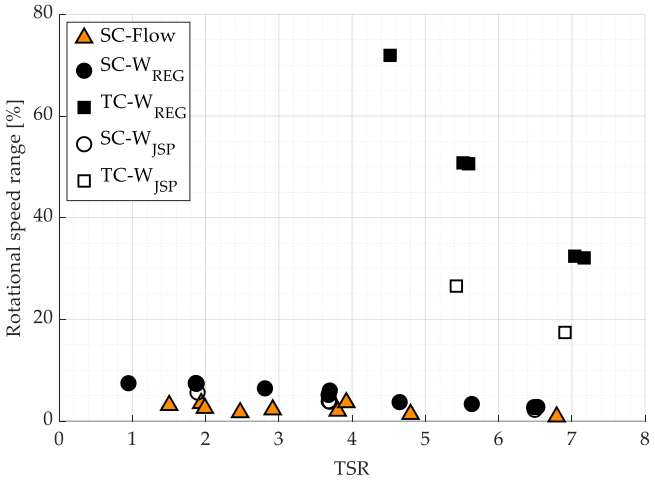

a)

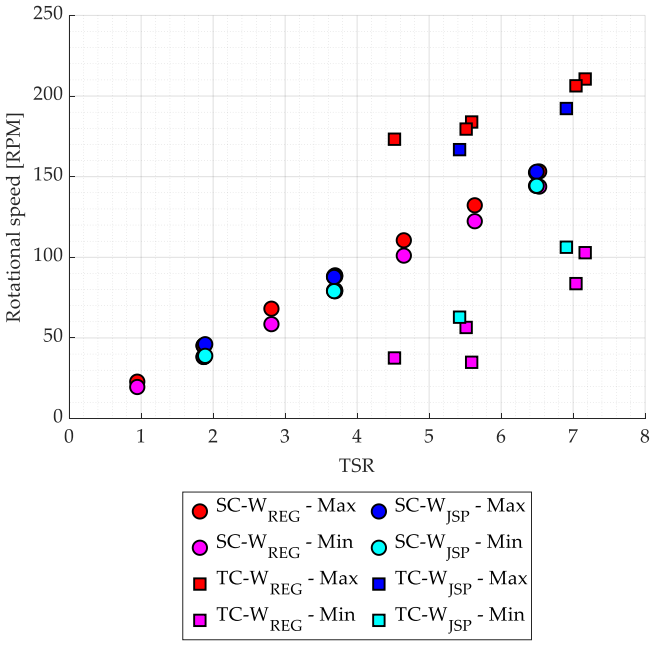

b)

Figure 7 Average turbine rotational speed fluctuation for all cases a) average fluctuation range b) average maximum and minimum rotational speeds.

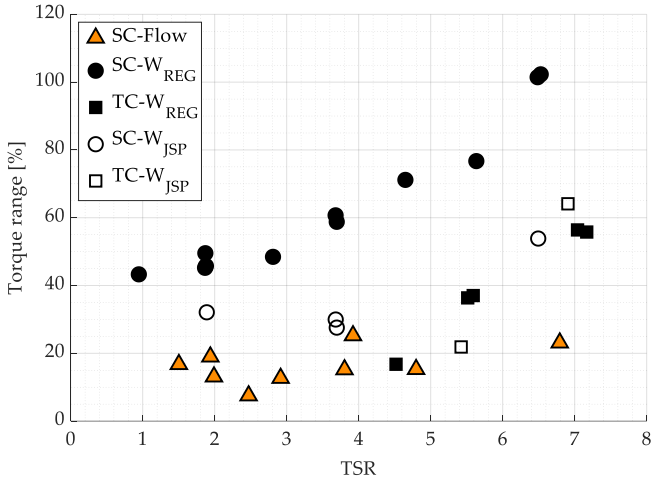

a)

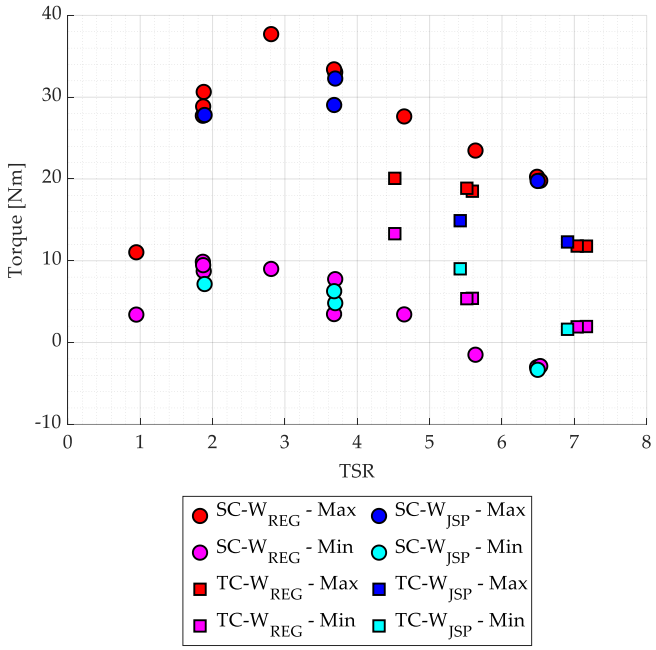

b)

Figure 8 Average torque fluctuation for all cases a) fluctuation range b) average maximum and minimum torque.

In Figure 8 the fluctuations in the torque signals are presented. For the speed control cases, there is an increase in the torque fluctuation range with TSR (Figure 8a), with a fluctuation range of up to 100% of the mean torque value in regular waves, 65% in irregular waves and 20% in flow only. For the torque control cases, for both regular and irregular waves, the torque range goes up to 60% from the mean torque values.

The maximum and minimum values of torque behave similarly in torque and speed control modes. They decrease as TSR increases with a dip on TSR=1. The range for speed control is roughly 30 Nm and 10 Nm for the torque control cases.

Thrust fluctuations are presented in Figure 9 for all cases. From the figure, it is clear that the torque control cases have a stronger influence on the thrust fluctuations than under speed control. The largest range observed (Figure 9a) in torque control mode is 75% of the mean thrust. In speed control this range was considerably smaller at 55% of the mean thrust. This ranges behave in

opposite manners. In the torque control case the range decreases with TSR while it increases with TSR for the speed control cases. At approximately TSR≈6.5 the two ranges of torque and speed control meet. From the slopes, it is anticipated that at higher TSR values the thrust fluctuations would increase for speed control and lower for torque control. It is unknown how high and low these values could become as the turbine was designed to have optimum performance at lower TSR values. At around TSR=4.5 the range difference between torque and speed control cases with regular waves is 35%.

Looking at Figure 9b, the fluctuation size in torque control mode appears to increase with TSR for the speed control cases but remains fairly unchanged for torque control cases. For the speed control cases, the minimum values stay approximately constant while the maximum values increase with TSR.

The influence of the control mode on the turbine behaviour is presented in Figure 7-9. It can be seen how the control mode impacts the design loads and fatigue response of the mechanical and structural components of the turbine. Speed control causes fluctuations in torque and thrust while torque control results in fluctuations in rotational velocity and thrust. From Figure 9, it can be concluded that applying a constant torque significantly increases the thrust fluctuations that the different turbine components must withstand. All the features presented in Figure 7, 8 and 9 are not exclusive to this facility as they all match with the features presented in [14].

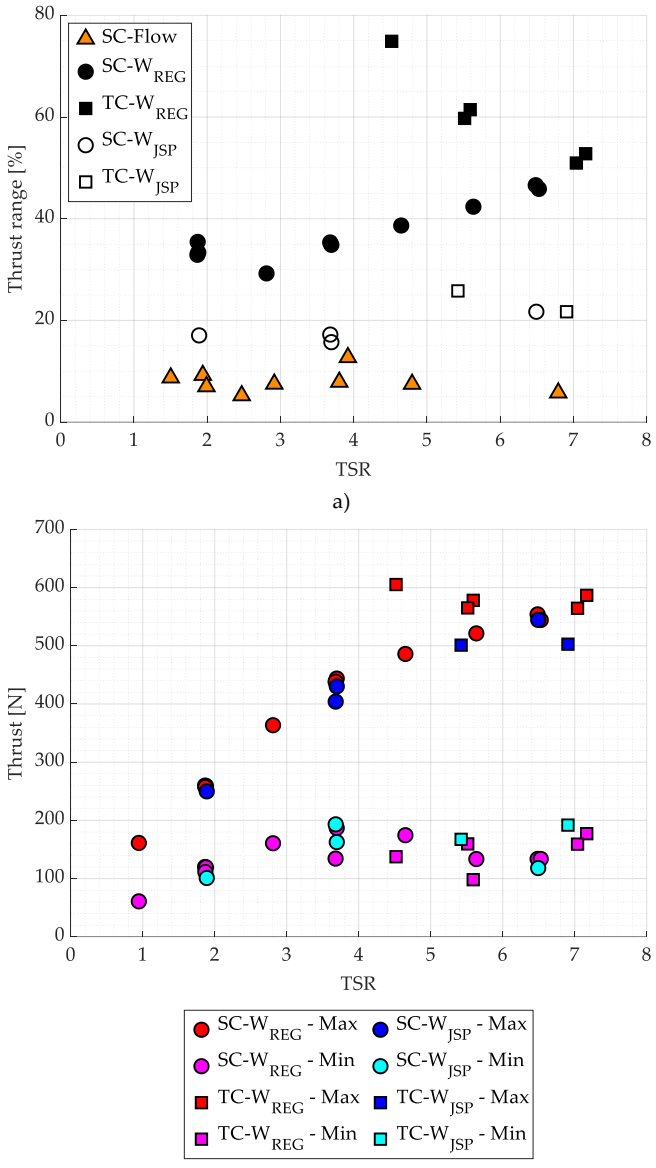

Figure 9 Average thrust fluctuation per wave period (speed and torque control cases) a) fluctuation range b) average maximum and minimum thrust per wave period

C. *Phasing of loading patterns*

In order to have a better understanding on how the waves interact with the turbine loadings, the time histories of the signals were investigated.

Following from [14], the phase difference between the turbine measurements and the water surface elevation was investigated. In Figure 10 this phase difference between thrust and water surface elevation is plotted as histograms for all regular wave cases. Figure 10a uses zero up-crossing method to calculate the phase difference while Figure 10b uses zero down-crossing. Regardless of the method, the phase difference observed is positive in its vast majority (20°), meaning that, in this case the thrust, is being "seen" by the turbine before the wave reaches the rotor.

The phase difference between thrust and water surface elevation is plotted against TSR in Figure 11. The phase difference has a concave shape, with the higher values at the lower TSRs and a minimum at TSR=4. From TSR=4, the phase difference starts increasing with TSR. There is

approximately a 5° smaller phase difference when operating with constant torque and variable speed.

The phase difference shown in Figure 11 means that each peak in the thrust signal occurs between approximately 5° and 30° before the peak in the surface elevation signal. This difference represents a significant lag between the two measurements. This is important to take into account when designing control strategies to reduce loading fluctuations.

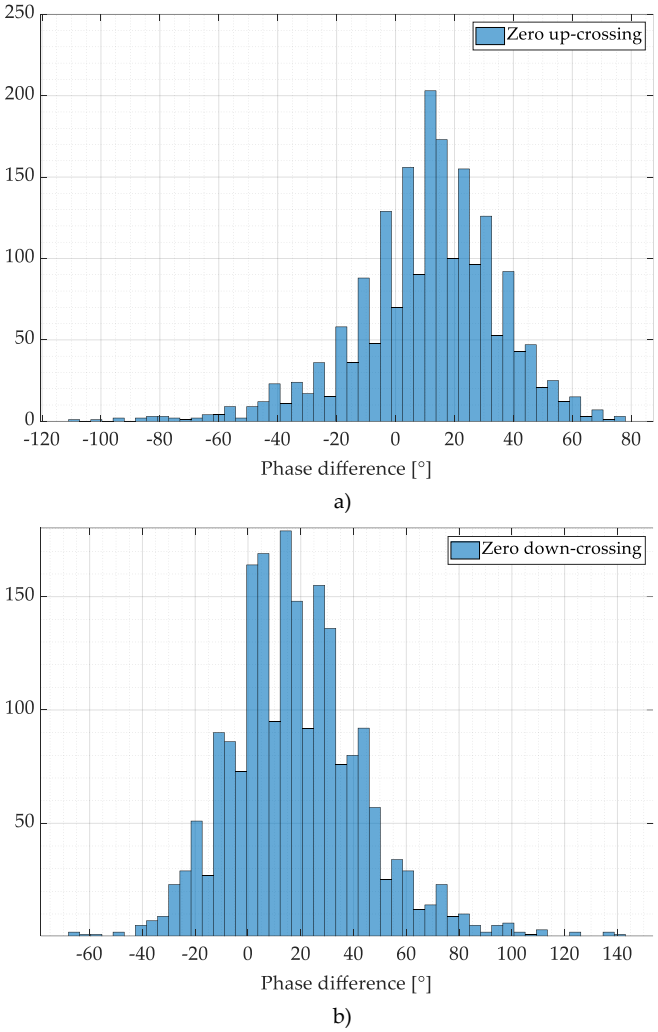

Figure 10 Histograms of phase difference between rotor thrust and water surface elevation signals for all regular wave cases. a) Zero up-crossing b) Zero down-crossing.

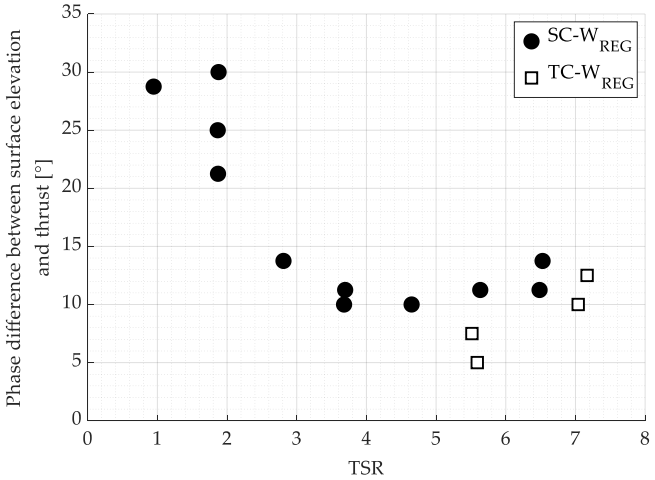

Figure 11 Phase difference between surface elevation and thrust for different TSR values.

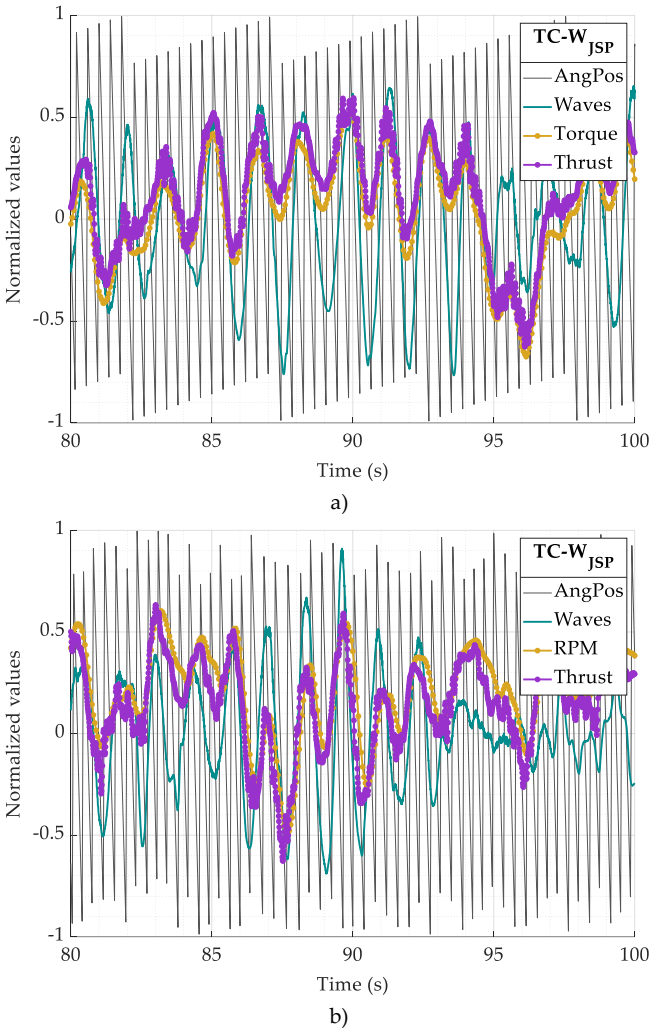

Figure 12 Comparison of water surface elevation, blade 1 position, rotor thrust, rotor torque (speed control only) and rotational velocity (torque control only) signals in irregular waves a) speed control b) torque control

The variability in the wave period of the irregular wave cases didn't allow for phase averaging as with the regular wave cases. Instead, the difference in the signals was investigated by plotting the signals side by side (Figure 12). Note that each signal has been re-scaled from -1 to 1 and centred so that its mean is equal to zero to provide easier comparison of the time series.

In contrast to findings in [14], it is not possible to see any phasing between the surface elevation and thrust signals. One of the main reasons is the recirculating nature and turbulence of the flume tank in comparison to the towing tank tests from [14].

Also noticeable in Figure 12 is that the torque, thrust and rotational velocity show a damping effect in relation to the water surface elevation signal. This effect could potentially be related to inertia of the turbine, so that small, quick fluctuations in the onset flow do not affect the rotational velocity nor the rotor loadings.

IV. CONCLUSIONS

Laboratory testing on a three bladed horizontal axis tidal turbine was performed at IFREMER's recirculating wave flume. Testing conditions included flow-only,

combined regular and irregular wave and current. All conditions were tested in speed and torque control. A transducer mounted at the end of the main drive shaft was used to measure rotor thrust and torque. The blade root bending moment was measured using strain gauges mounted on the blade fittings. The main conclusions from the study are:

- Controlled parameters (torque and rotational speed) showed small standard deviations
- Average turbine load values remained unchanged between control modes
- Average turbine load values remained unchanged with superposition of waves
- Under torque control, the average thrust range was around 75% higher than the mean value.
- Thrust fluctuates from its mean value over a range 35% larger under torque control than under speed control.
- A phase difference between the water surface elevation signal and the thrust, torque and rotational speed signals was observed. This phase difference changes as TSR increases in a concave manner. In this case, the phase difference means that the fluctuations in torque, thrust and rotational speed happen instants before the waves passage.
- At similar TSR, phase difference under torque control showed a 5-degree reduction between the rotor thrust and water surface elevation signals compared to speed control.
- In irregular waves there was no significant phase difference identified but looking into the time series showed that thrust, torque and rotational speed signals behave like a dampened version of the water surface elevation signal.

Future work includes a further week of testing at IFREMER's recirculating tank, another week at FloWave's circular recirculating tank, another week at Strathclyde's tow tank and possibly going back to INSEAN's tow tank. These further testing will help confirm findings present here and in [14] and [15] and to extend the test plan to include more repeats of tests already conducted as well as array testing. These tests are part of the DyLoTTA project due for completion in late 2019. The results will serve as input for numerical modelling as part of the DyLoTTA project as well as providing new insights and confirming previous knowledge into wave-current loading on tidal turbines.

ACKNOWLEDGMENT

This laboratory study was funded under the MARINET2 programme as part of the DyLoTTA Supergen UKCMER Grand Challenge Project funded by the EPSRC. The authors would like to thank the staff at IFREMER for their expertise and support during the testing period.

REFERENCES

[1] B. Gaurier, P. Davies, A. Deuff, and G. Germain, "Flume tank characterization of marine current turbine blade behaviour under current and wave loading," *Renew. Energy*, vol. 59, pp. 1–12, 2013.

[2] N. Barltrop, K. S. Varyani, A. D. Grant, D. Clelland, and X. P. Pham, "Investigation into wave—current interactions in marine current turbines," *Proc. Inst. Mech. Eng. Part A J. Power Energy*, vol. 221, no. 2, pp. 233–242, Mar. 2007.

[3] T. A. de Jesus Henriques *et al.*, "The effects of wave-current interaction on the performance of a model horizontal axis tidal turbine," *Int. J. Mar. Energy*, vol. 8, no. December 2014, pp. 17–35, 2014.

[4] P. W. Galloway, L. E. Myers, and A. S. Bahaj, "Studies of a scale tidal turbine in close proximity to waves," *Proc. 3rd Int. Conf. Ocean Energy*, no. 1, pp. 3–8, 2010.

[5] S. Ordonez-Sanchez, K. Porter, C. H. Frost, M. Allmark, C. M. Johnstone, and T. O'Doherty, "Effects of Wave-Current interactions on the performance of tidal stream turbines," in *Proceedings of the 3rd Asian Wave and Tidal Energy Conference*, 2016, pp. 978–981.

[6] R. Martinez, G. S. Payne, and T. Bruce, "The effects of oblique waves and current on the loadings and performance of tidal turbines," *Ocean Eng.*, 2017.

[7] S. Draycott, A. Nambiar, B. Sellar, T. Davey, and V. Venugopal, "Assessing extreme loads on a tidal turbine using focused wave groups in energetic currents," *Renew. Energy*, vol. 135, pp. 1013–1024, 2019.

[8] S. Draycott, G. Payne, J. Steynor, A. Nambiar, B. Sellar, and V. Venugopal, "An experimental investigation into non-linear wave loading on horizontal axis tidal turbines," *J. Fluids Struct.*, vol. 84, pp. 199–217, 2019.

[9] T. M. Nevalainen, "The effect of unsteady sea conditions on tidal strea mturbine loads and durability," Strathclyde University, 2016.

[10] H. R. Mullings, T. J. Stallard, and G. S. Payne, "Operational Loads On A Tidal Turbine due to Environmental Conditions," in *Proceedings of the International Offshore and Polar Engineering Conference*, 2017, no. June.

[11] S. C. Tatum, M. Allmark, C. H. Frost, D. M. O'Doherty, A. Mason-Jones, and T. O'Doherty, "CFD Modelling of a Tidal Stream Turbine Subjected to Profiled Flow and Surface Gravity Waves," in *Proceedings of the 11th European Wave and Tidal Energy Conference*, 2015, pp. 1–10.

[12] T. M. Nevalainen, C. M. Johnstone, and A. D. Grant, "A sensitivity analysis on tidal stream turbine loads caused by operational, geometric design and inflow parameters," *Int. J. Mar. Energy*, vol. 16, pp. 51–64, Dec. 2016.

[13] M. A. Holst, O. G. Dahlhaug, and C. Faudot, "CFD Analysis of Wave-Induced Loads on Tidal Turbine Blades," *IEEE J. Ocean. Eng.*, no. April 2016, 2014.

[14] K. Porter *et al.*, "Laboratory Study of Tidal Turbine Performance in Irregular Waves," in *Proceedings of the 4th Asian Wave and Tidal Energy Conference*, 2018.

[15] S. Ordonez-Sanchez *et al.*, "Analysis of a Horizontal Axis Tidal Turbine Performance in the Presence of Regular and Irregular Waves using Two Control Strategies," *J. Mar. Sci. Eng.*, vol. Under Revi, 2019.

[16] M. Allmark, R. Ellis, K. Porter, T. O. Doherty, and C. Johnstone, "The Development and Testing of a Lab-Scale Tidal Stream Turbine for the Study of Dynamic Device Loading," in *Proceedings of the 4th Asian Wave and Tidal Energy Conference*, 2018.

[17] M. Allmark, "Condition monitoring and fault diagnosis of tidal stream turbines subjected to rotor imbalance faults," Cardiff University, 2016.

[18] A. Mason-Jones, "Performance assessment of a horizontal axis tidal turbine in a high velocity shear environment," Cardiff University, 2010.

[19] R. Ellis *et al.*, "Design Process for a Scale Horizontal Axis Tidal Turbine Blade .," in *Proceedings of the 4th Asian Wave and Tidal Energy Conference*, 2018.

[20] T. Burton, N. Jenkins, D. Sharpe, and E. Bossanyi, *Wind Energy Handbook*. 2011.